

# First-order phase transition in MnAs disks on GaAs (001)

Y. Takagaki, B. Jenichen, C. Herrmann, E. Wiebicke, L. Däweritz, and K. H. Ploog  
*Paul-Drude-Institut für Festkörperelektronik, Hausvogteiplatz 5-7, 10117 Berlin, Germany*

(Received 25 January 2006; published 20 March 2006)

Size effects on a first-order phase transition in submicron disks is demonstrated using a high-resolution imaging method. In MnAs disks on GaAs (001) substrates having sizes smaller than twice the film thickness, an individual disk consists of either entirely  $\alpha$ -MnAs or entirely  $\beta$ -MnAs as a consequence of the nucleation initiation of the first-order phase transition. A phase coexistence occurs on macroscopic scales as the two kinds of the disks can be present simultaneously. In slightly larger disks, the stripe structure due to the phase coexistence in films is modified to a core-shell type phase segregation.

DOI: [10.1103/PhysRevB.73.125324](https://doi.org/10.1103/PhysRevB.73.125324)

PACS number(s): 75.75.+a, 64.70.Nd, 05.70.Fh, 61.46.-w

## I. INTRODUCTION

The simultaneous structural and magnetic phase transition in bulk MnAs at the critical temperature  $T_c \approx 40^\circ\text{C}$  has been investigated in detail.<sup>1,2</sup> The low-temperature phase,  $\alpha$ -MnAs, is ferromagnetic having hexagonal crystal structure. Above  $T_c$ , the crystal structure transforms into orthorhombic<sup>3</sup> and the material,  $\beta$ -MnAs, loses the ferromagnetism.<sup>4</sup> The phase transition is first order; i.e., the transition is abrupt and displays a temperature hysteresis.<sup>2</sup>

The material properties of MnAs in epitaxial thin films and microstructures have become an important subject in the last decade due to “spintronics” applications.<sup>5,6</sup> In films grown on GaAs substrates, the two phases coexist for a wide temperature range around  $T_c$ .<sup>7,8</sup> The coexistence is governed by the combination of two types of stresses:<sup>8</sup> phase transition stress due to an abrupt volume change at the phase transition and thermal stress due to the unusually large thermal expansion of MnAs. During growth of MnAs layers, most of the lattice mismatch between MnAs and GaAs is compensated by introducing misfit dislocations. Upon cooling the MnAs/GaAs heterostructures towards room temperature,<sup>9</sup> the MnAs films are tensile strained as the thermal expansion of MnAs is one order of magnitude larger than that of GaAs.<sup>10</sup> When the temperature is lowered beyond  $T_c$ , however, the MnAs films suddenly experience additional compressive strain, as the phase transition from the  $\beta$  phase to the  $\alpha$  phase involves a volume expansion.<sup>11</sup> The discontinuous volume change favors a mixture of the two phases rather than a homogeneously stressed uniform phase as the system saves the strain energy by balancing the stresses. The fractions of the two phases vary continuously over a certain interval of temperature, typically 20–30 °C in MnAs/GaAs (001) structures.<sup>8</sup> The coexistence temperature regime shifts to the high- or low-temperature side of  $T_c$  depending on whether the tensile strain due to the thermal expansion mismatch or the compressive strain due to the volume change is dominant, respectively.

For GaAs (001) substrates,<sup>12</sup> the phase coexistence leads to the formation of a quasiperiodic stripe structure<sup>13</sup> [see Fig. 1(a)]. The MnAs films grow with the (1 $\bar{1}$ 00) plane as the surface plane. The [0001] and [11 $\bar{2}$ 0] directions of MnAs are aligned along the [1 $\bar{1}$ 0] and [110] directions of GaAs, respectively. The sudden change of the lattice constants of

MnAs at the phase transition occurs in the [11 $\bar{2}$ 0] and [1 $\bar{1}$ 00] directions, whereas the lattice constant in the [0001] direction is almost unchanged. As a consequence, narrow strips of  $\alpha$ - and  $\beta$ -MnAs alternate in the MnAs [11 $\bar{2}$ 0] direction so as to cancel out the phase-transition and thermal stresses.<sup>8</sup> The stress remains intact along the MnAs [0001] direction as there is no compensation mechanism for that direction.<sup>14</sup> The stripes give rise to a height modulation with a magnitude of a few nm. The period  $d$  of the stripes increases almost linearly with the layer thickness  $t$ , exhibiting a relationship  $d \approx 4.8t$ .<sup>15</sup> For typical values of  $t$  ( $\sim 100$  nm),  $d$  is about a half  $\mu\text{m}$ , which is the size that allows us to enforce artificial constraints on the phase transition using microfabrication technologies.

In this paper, we report on the phase transition when MnAs films are processed to disks having lateral dimensions comparable to or less than the period  $d$ . The distribution of phase domains in microstructures is imaged with a high spatial resolution using scanning probe microscopies. While the two phases remain to coexist irrespective of the size of the disks, the nature of the coexistence is found to be affected fundamentally by the size reduction.

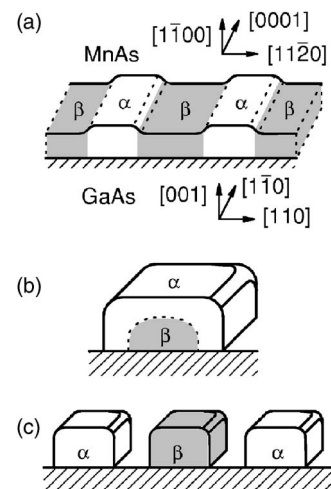


FIG. 1. Schematic of the phase coexistence in MnAs films (a) and disks (b), (c) on GaAs (001). (b) and (c) correspond to the disks having the size comparable to and significantly smaller than the period of the stripes of  $\alpha$ -MnAs and  $\beta$ -MnAs in the film, respectively.

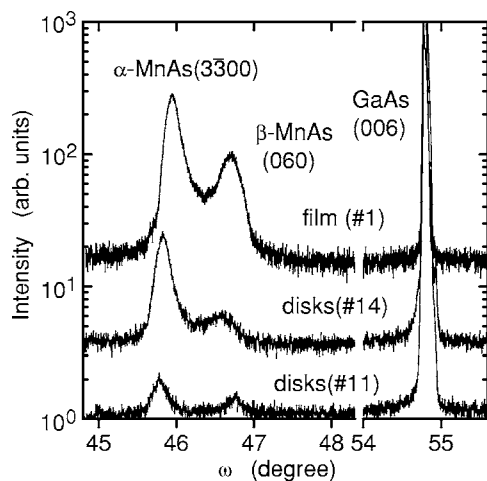


FIG. 2. X-ray diffraction curves ( $\omega$ - $2\theta$  scan) of a MnAs film (No. 1) on GaAs (001) and disks (Nos. 14 and 11) fabricated from the film at 29 °C using Cu  $K\alpha_1$  radiation. The three peaks are associated with the GaAs (006),  $\alpha$ -MnAs( $\bar{3}\bar{3}00$ ), and  $\beta$ -MnAs (060) reflections. The bars indicate the position of the peaks for the film. The curves are offset for clarity.

## II. SAMPLE PREPARATION AND X-RAY-DIFFRACTION ANALYSIS

Two high-quality MnAs films were grown on GaAs (001) substrates at 230 °C by molecular-beam epitaxy.<sup>13</sup> We refer to the films as Nos. 1 and 2. The film thickness was 50 nm for both samples. The MnAs layer for No. 2 was grown on a GaAs buffer layer that included a buried  $\text{Al}_{0.3}\text{Ga}_{0.7}\text{As}$  layer. The embedded layer gave rise to a significantly lower  $\alpha$ -phase fraction ( $\approx 40\%$ ) in the film than that ( $\approx 70\%$ ) in film No. 1, plausibly due to a modification of the strain between the epilayer and substrate. The MnAs disks were fabricated from the epitaxial films using electron-beam lithography and Ar-ion milling. As the etch rate for MnAs is significantly smaller than that for GaAs, the etching proceeded typically about 100 nm deep into the GaAs substrate; i.e., MnAs disks were placed on top of GaAs pillars. The shape of the disks was either circular (for small disks), square (for large disks), or square with rounded corners (generally for medium-size disks). The disks were assembled in the form of a square array. We note that the magnetic interaction among the disks is negligibly small.

In Fig. 2, we show x-ray-diffraction (XRD) curves ( $\omega$ - $2\theta$  scan with  $\omega$  being the glancing angle of incidence on the sample surface and  $2\theta$  the detector angle with respect to the incident beam) of film No. 1 and the disks fabricated from it at 29 °C. In addition to the GaAs (006) peak originating from the substrate, two peaks associated with the MnAs layer are present.<sup>8</sup> They are identified to be due to the  $\alpha$ -MnAs ( $\bar{3}\bar{3}00$ ) and  $\beta$ -MnAs (060) reflections.<sup>16</sup> Based on the relative intensities of the two peaks and the ratio of their structure factors, the fractions of the  $\alpha$  and  $\beta$  phases of MnAs can be estimated. For the film in Fig. 2, for instance, 71% of MnAs is indicated to be in the  $\alpha$  phase.

The curves in Fig. 2 for the MnAs disks, having the sizes of 430 and 100 nm, reveal two immediate findings. (i) The

TABLE I.  $\alpha$ -phase fraction at 29 °C estimated using x-ray diffraction in two films and the disks fabricated from them. The size of the disks and the period of the disk arrays were determined from scanning-electron micrographs.

Sample No.	Size (nm)	Array period (nm)	$\alpha$ -phase fraction (%)
1	film		71
11	100	390	76
12	170	750	78
13	220	390	81
14	430	760	87
15	800	1450	72
2	film		42
21	75	390	38
22	90	390	87
23	95	400	49
24	140	520	58

amount of the  $\alpha$  phase increases in the disks. The  $\alpha$ -phase fraction for various sizes of the disks is summarized in Table I. (ii) The shift in the position of the  $\alpha$ -MnAs ( $\bar{3}\bar{3}00$ ) peak indicates that the lattice constant of  $\alpha$ -MnAs enlarges in the direction normal to the surface. The sizes of the smallest disks are significantly less than the period of the  $\alpha$ - $\beta$  stripes, which is 220 nm as determined by atomic-force microscopy (AFM), so that the stripe structure can no longer be accommodated within the disks. In addition, the exposed side walls of the disks help to relax the stress. It was observed in Ref. 14 that the  $\beta$ -MnAs segments in the stripe structure were converted to the ferromagnetic phase when the adjacent  $\alpha$ -MnAs segments were removed by a phase-selective wet chemical etching. One may hence expect an abrupt transition between  $\alpha$ -MnAs and  $\beta$ -MnAs which is inherent for the first-order phase transition to be restored in such small disks. That is, the MnAs in the small disks should transform entirely into the  $\alpha$  phase at room temperature. Although  $\alpha$ -MnAs increased its fraction in all but one disk, the existence of both phases is apparent (see Table I), contrary to this expectation. As the initial phase fractions in the two films are significantly different, the phase coexistence in small disks is evidenced to be generic.

## III. MAGNETIC-FORCE MICROSCOPY

In order to clarify the mechanism for the coexistence of the two phases within disks, we examined the magnetic properties of the disks using magnetic-force microscopy (MFM). We exploit the advantage that the distribution of  $\alpha$ - and  $\beta$ -MnAs can be determined as the regions of ferromagnetic and nonmagnetic components. We note that the phase distribution of first-order phase transitions has been studied typically using an optical microscope,<sup>17</sup> for which the spatial resolution is limited to micron scales. Our approach allows us to study the phase transitions with a high resolution.

In Figs. 3(b) and 4(b), we show MFM images of the MnAs disks having the sizes of 170 and 100 nm, respec-

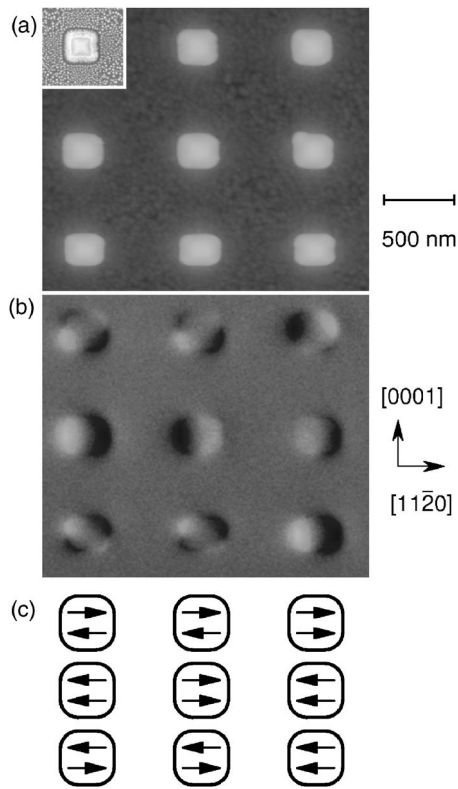


FIG. 3. Atomic-force (a) and magnetic-force (b) micrographs of 170-nm-large disks (No. 12) at 25 °C. The upper-left image in (a) is the scanning-electron micrograph of a typical disk. The horizontal thick arrows in (c) indicate the magnetization direction of the double magnetic domain in the disks, in correspondence to the image in (b).

tively. In our MFM setup, the magnetic field normal to the surface is detected by a scanning tip. The bright and dark contrasts in the MFM images correspond to the areas where the magnetic fields are directed out of and towards the surface plane, respectively. In identifying the ferromagnetic regions in the MFM images, it is important to understand the magnetic-domain structure in submicron disks.<sup>18</sup> While the magnetic moments lie within the surface plane as a result of the shape anisotropy, ferromagnetic disks exhibit a transition from multiple magnetic domains to single magnetic domain upon reducing the disk diameter. When the diameter is larger than a critical value, the magnetic structure of the disks is a closure-flux-type multidomain state. In disks smaller than the critical size, in contrast, the domain-wall energy exceeds the magnetostatic energy arising from stray fields. Thus, each disk consists of a single magnetic domain even in a demagnetized state. As we demonstrate below, the critical size for the single-magnetic-domain regime is around 100 nm for the present MnAs disks.

The five disks contained in the middle row and the right-hand-side column in Fig. 3(b) possess a single magnetic moment with its direction as illustrated in Fig. 3(c). (The magnetization direction is indicated by two arrows due to the reason that will soon become clear below.) Due to the extremely large uniaxial magnetocrystalline anisotropy in MnAs films,<sup>7,19</sup> these single magnetic moments are always

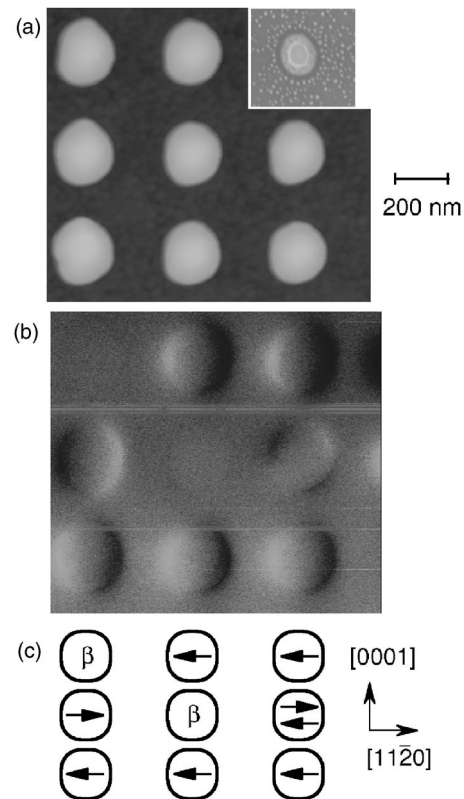


FIG. 4. Atomic-force (a) and magnetic-force (b) micrographs of 100-nm-large disks (No. 11) at 25 °C. The upper-right image in (a) is the scanning-electron micrograph of a typical disk. The phase (for the  $\beta$ -MnAs disks) or the magnetization direction (for the  $\alpha$ -MnAs disks) of the disks corresponding to the image in (b) is illustrated in (c).

oriented along the magnetic easy axis, which lies along the MnAs  $[11\bar{2}0]$  direction. The rest of the four disks in Fig. 3(b) exhibit two magnetic domains with antiparallel magnetization orientation. The multidomain states in disks that are somewhat larger than the critical size contain no more than two magnetic domains due, again, to the huge uniaxial anisotropy. This is in contrast to the fourfold-symmetric domains observed in the disks processed from roughly isotropic ferromagnetic films, such as Fe and Co.<sup>20</sup>

Out of 44 disks observed in No. 12, 23 disks exhibited the antiparallel configuration. The numbers of the disks that showed a single magnetic moment pointing to the left and right were both 10. (One disk vanished in the MFM image. We will return to this phenomenon later.) That the numbers of the left- and right-pointing disks are identical is a consequence of the sample having been intentionally demagnetized prior to the MFM imaging by heating it to  $\sim 60$  °C, at which MnAs becomes entirely the nonmagnetic  $\beta$  phase. The fact that almost half the demagnetized disks exhibit antiparallel magnetic moments implies that the 170-nm-large disks are in the double-domain state with the magnetic moments being directed randomly. The configuration of the single magnetic moment was obtained when the magnetization directions of both domains were the same by coincidence.

Despite the considerable amount of  $\beta$ -MnAs indicated by the XRD curve, the identical size of the image of the disks

taken by MFM and that obtained by the same scanning tip in the AFM mode, Fig. 3(a), reveals that the entire top surface of the disks consists of ferromagnetic  $\alpha$ -MnAs. [We note that the disks appeared larger in MFM and AFM images than in the scanning-electron micrograph, which is shown at the upper-left corner in Fig. 3(a), as the height of the etched MnAs/GaAs pillars was too large for the scanning-tip microscopies to enable faithful imaging of the disk size. The size difference is even more pronounced in Fig. 4(a) as the disk diameter is smaller than the pillar height.] Therefore,  $\beta$ -MnAs is indicated to be buried underneath, plausibly in the vicinity of the MnAs-GaAs interface as illustrated in Fig. 1(b). On the one hand, the stress-free surface MnAs is in the  $\alpha$  phase as  $T_c$  of bulk MnAs is above room temperature.<sup>14</sup> The additional surface area at the side of the disks after the microstructuring leads to an increase of the  $\alpha$ -phase fraction, as observed by XRD. On the other hand, the interior of the disk will be kept under a significant stress by the substrate, thereby stabilizing the  $\beta$  phase. The expansion of the lattice in the vertical direction indicated by the XRD curves for the disks in Fig. 2 may be regarded as evidence that the MnAs disks are not completely free of stress even in the smallest disks, since the suppression of the compressive strain in the in-plane direction by the microstructuring should result in a contraction of the lattice in the vertical direction. Therefore, the phase coexistence persists by modifying the distribution of the two phases to the core-shell-like configuration. The redistribution of the two phases has a serious consequence when microstructured MnAs is employed as, for instance, spin injectors and detectors since the nonmagnetic phase is placed at the MnAs-GaAs interface.<sup>6</sup>

The situation is markedly different when the disk size is 100 nm (No. 11). Many of the disks are characterized by a single magnetic moment. Among the 50 disks we examined, 26 and 6 disks indicated a single magnetic domain with the magnetization pointing to left and right, respectively. (The sample was again intentionally demagnetized prior to the MFM imaging.) The antiparallel-double-domain feature was observed only in 10 disks. As the number of single-magnetic-domain disks is well more than that expected for the coincidental alignment of two magnetic moments, the critical disk size for the transition between the multiple- and single-magnetic-domain regimes is indicated to be around 100 nm. Moreover, the most striking feature in No. 11 is that as many as 8 disks (16% of the total number of the disks) are not visible in the MFM image. Notice the two missing disks of the array in Fig. 4(b). Only 1 out of 44 disks similarly disappeared in the MFM image from No. 12. If the magnetic domain is of a vortex type, the magnetic contrast would be weak owing to the few stray fields. Given the gigantic uniaxial anisotropy in MnAs films, however, it is very unlikely that the magnetic moments can tilt away from the easy axis. In MnAs wires with a width only about twice the layer thickness, the magnetization direction remained undisturbed even though the wires were stretched perpendicular to the easy axis.<sup>14</sup> This corroborates that the uniaxial magnetocrystalline anisotropy overwhelms the shape anisotropy. We therefore conclude that the vanished disks are fully occupied by the  $\beta$  phase. These disks already account for two-thirds of the  $\beta$ -MnAs shown to be present by the XRD curve. We

presume that most of the rest of the disks—i.e., the ferromagnetic disks—consist completely of  $\alpha$ -MnAs.

The two phases of MnAs no longer share a single disk when the disk size is smaller than 100 nm. The phase transition within a disk is hence indeed abrupt. Nevertheless, the phase coexistence survives on a macroscopic scale. The disks are divided to those composed of  $\alpha$ -MnAs and those composed of  $\beta$ -MnAs instead of the phase of all the disks being driven to a favored one. It is reasonable to assume that the number counting of the  $\alpha$ -MnAs disks and the  $\beta$ -MnAs disks yields the phase fractions expected for the ordinary phase coexistence in films, provided that the reduced stress due to the increased surface areas is properly accounted for to increase the  $\alpha$ -phase fraction.

The simultaneous presence of the  $\alpha$ -phase disks and the  $\beta$ -phase disks is a manifestation of the nucleation initiation of the first-order phase transition of MnAs. While the temperature crosses  $T_c$  to the condition corresponding to a new phase, a first-order phase transition does not occur immediately. The system stays in a metastable state until nuclei are formed by surmounting the potential barrier separating the phases. The nuclei are favored and thus grow further until a macroscopic phase transition has been realized. Since the disks in the array are independent from each other, whether each disk maintains its existence in the metastable phase or changes to the stable phase is a stochastic process. The disks can be in either phase with a certain probability. Although the phase transition in the small disks hence resembles that in a bulk, we emphasize that the metastable states appear to be stabilized by the stress from the substrate.<sup>21</sup> The temperature range for the thermal hysteresis in a bulk MnAs is above room temperature.<sup>2</sup> This explains the observation in Fig. 3 that the surface MnAs is almost completely in the  $\alpha$  phase. The fairly large number of  $\beta$ -MnAs disks at room temperature, therefore, highlights an undiminished influence of the substrate.

#### IV. CONCLUSION

In conclusion, we have investigated the phase transition between the  $\alpha$  and  $\beta$  phases of MnAs in a mesoscopic system using a high-resolution imaging method. In medium-size disks, the phase coexistence persists by adopting a core-shell-type phase segregation. When the disk size is further reduced, the phase distribution is “quantized” to a particle like behavior, in reminiscence of the photons in the distribution of light intensities. Individual disks are required to be either entirely in the  $\alpha$  phase or entirely in the  $\beta$  phase due to the nucleation initiation of the first-order phase transition of MnAs. However, one can predict only the probability of the phase for a single disk. A macroscopic phase coexistence remains as a supersaturation. The size effects are thus demonstrated to alter the nature of the phase transition in nanometer-scale disks.

#### ACKNOWLEDGMENT

Part of this work was supported by the Federal Ministry of Education and Research (nanoQUIT program).

- <sup>1</sup>R. W. de Blois and D. S. Rodbell, Phys. Rev. **130**, 1347 (1963); A. Stoffel, J. Schneider, and F. Hartmann, IEEE Trans. Magn. **6**, 545 (1970).
- <sup>2</sup>H. Okamoto, Bull. Alloy Phase Diagrams **10**, 549 (1989).
- <sup>3</sup>R. H. Wilson and J. S. Kasper, Acta Crystallogr. **176**, 95 (1964).
- <sup>4</sup>There is a debate whether  $\beta$ -MnAs is paramagnetic or antiferromagnetic. See M. K. Niranjana, B. R. Sahu, and L. Kleinman, Phys. Rev. B **70**, 180406(R) (2004) and H. Yamaguchi, A. K. Das, A. Ney, T. Hesjedal, C. Pampuch, D. M. Schaadt, and R. Koch, Europhys. Lett. **72**, 479 (2005).
- <sup>5</sup>M. Tanaka, Semicond. Sci. Technol. **17**, 327 (2002).
- <sup>6</sup>M. Ramsteiner, H. Y. Hao, A. Kawaharazuka, H. J. Zhu, M. Kästner, R. Hey, L. Däweritz, H. T. Grahn, and K. H. Ploog, Phys. Rev. B **66**, 081304(R) (2002).
- <sup>7</sup>F. Schippan, G. Behme, L. Däweritz, K. H. Ploog, B. Dennis, K.-U. Neumann, and K. R. A. Ziebeck, J. Appl. Phys. **88**, 2766 (2000).
- <sup>8</sup>V. M. Kaganer, B. Jenichen, F. Schippan, W. Braun, L. Däweritz, and K. H. Ploog, Phys. Rev. Lett. **85**, 341 (2000); Phys. Rev. B **66**, 045305 (2002).
- <sup>9</sup>MnAs exhibits a second-order structural phase transition at 125 °C. This phase transition can be ignored in considering the thermal stress as the thermal expansion of the third phase,  $\gamma$ -MnAs, and  $\beta$ -MnAs is similar.
- <sup>10</sup>B. T. M. Willis and H. P. Rooksby, Proc. Phys. Soc. London, Sect. B **67**, 290 (1954).
- <sup>11</sup>C. P. Bean and D. S. Rodbell, Phys. Rev. **126**, 104 (1962).
- <sup>12</sup>M. Tanaka, J. P. Harbison, T. Sands, T. L. Cheeks, V. G. Keramidas, and G. M. Rothberg, J. Vac. Sci. Technol. B **12**, 1091 (1994).
- <sup>13</sup>M. Kästner, C. Herrmann, L. Däweritz, and K. H. Ploog, J. Appl. Phys. **92**, 5711 (2002).
- <sup>14</sup>Y. Takagaki, E. Wiebicke, T. Hesjedal, H. Kostial, C. Herrmann, L. Däweritz, and K. H. Ploog, Appl. Phys. Lett. **83**, 2895 (2003).
- <sup>15</sup>L. Däweritz, L. Wan, B. Jenichen, C. Herrmann, J. Mohanty, A. Trampert, and K. H. Ploog, J. Appl. Phys. **56**, 5056 (2004).
- <sup>16</sup>B. Jenichen, V. M. Kaganer, C. Herrmann, L. Wan, L. Däweritz, and K. H. Ploog, Z. Kristallogr. **219**, 201 (2004).
- <sup>17</sup>J. F. Dillon, Jr., E. Yi Chen, N. Giordano, and W. P. Wolf, Phys. Rev. Lett. **33**, 98 (1974).
- <sup>18</sup>M. Hehn, K. Ounadjela, J.-P. Bucher, F. Rousseaux, D. Decanini, B. Bartenlian, and C. Chappert, Science **272**, 1782 (1996); R. P. Cowburn, D. K. Koltsov, A. O. Adeyeye, M. E. Welland, and D. M. Tricker, Phys. Rev. Lett. **83**, 1042 (1999).
- <sup>19</sup>Y. Takagaki, C. Herrmann, E. Wiebicke, J. Herfort, L. Däweritz, and K. H. Ploog, Appl. Phys. Lett. **88**, 032504 (2006).
- <sup>20</sup>M. Hanson, C. Johansson, B. Nilsson, P. Isberg, and R. Wäppling, J. Appl. Phys. **85**, 2793 (1999).
- <sup>21</sup>N. Menyuk, J. A. Kafalas, K. Dwight, and J. B. Goodenough, Phys. Rev. **177**, 942 (1969).